

# Microstructure and electric properties of lead-free $0.8\text{Bi}_{1/2}\text{Na}_{1/2}\text{TiO}_3\text{--}0.2\text{Bi}_{1/2}\text{K}_{1/2}\text{TiO}_3$ ceramics

Wei-Jing Ji<sup>a,\*</sup>, Yan-Bin. Chen<sup>b</sup>, Shan-Tao Zhang<sup>a</sup>, Bin Yang<sup>c</sup>, Xiao-Ning Zhao<sup>b</sup>, Qian-Jin Wang<sup>a</sup>

<sup>a</sup> National Laboratory of Solid State Microstructure and Materials Science, Engineering Department, Nanjing University, Hankou Road 22, Nanjing 210093, China

<sup>b</sup> National Laboratory of Solid State Microstructure, Physics Department, Nanjing University, Nanjing 210093, China

<sup>c</sup> Center for Condensed Matter Science and Technology, Department of Physics, Harbin Institute of Technology, Harbin 150001, China

Received 15 September 2011; received in revised form 28 September 2011; accepted 28 September 2011

Available online 5 October 2011

## Abstract

The microstructure and electric properties of the rhombohedral–tetragonal morphotropic phase boundary (MPB) composition  $0.8\text{Bi}_{1/2}\text{Na}_{1/2}\text{TiO}_3\text{--}0.2\text{Bi}_{1/2}\text{K}_{1/2}\text{TiO}_3$  have been investigated. X-ray and electron diffraction results substantiate the co-existence of tetragonal and rhombohedral phases. The ferroelectric domains were clearly observed by electron microscopy. The oxygen octahedron tilting of the samples was studied by SAED. Both saturated polarization–electric field and butterfly shaped strain–electric field hysteresis loops prove that the MPB composition shows typical ferroelectric nature. The detailed microstructure–property characterization may shed light on the physical property of further work on BNT–BKT around morphotropic phase boundary.

© 2011 Elsevier Ltd and Techna Group S.r.l. All rights reserved.

**Keywords:** BNT ceramics; Microstructure; TEM

## 1. Introduction

The study of lead-free piezoelectric ceramics has attracted much attention, and has been accelerated dramatically by the world-wide stringent regulations on the use of lead-based ceramics to protect the environments [1–3]. Morphotropic phase boundary (MPB) between two end members with different crystal structure is important for developing high performance piezoelectric ceramics, it is generally accepted that at the MPB the increased number of possible polarization variants is responsible for the enhanced piezoelectric properties. So far the reported lead-free piezoelectric ceramics are mainly based on  $\text{BaTiO}_3$  (BT),  $(\text{Bi},\text{Na})\text{TiO}_3$  (BNT), and  $(\text{K},\text{Na})\text{NbO}_3$  (KNN) and many compositions near MPB have been developed [2,3]. Among the materials based on BNT, the rhombohedral–tetragonal MPB compositions of  $(1.0-x)\text{Bi}_{1/2}\text{Na}_{1/2}\text{TiO}_3\text{--}x\text{Bi}_{1/2}\text{K}_{1/2}\text{TiO}_3$  ((1-x)BNT–xBKT, when  $x$  is 0.16–0.20) demonstrate superior piezoelectric property [4]. Based on this MPB, several ternary systems such as BNT–BKT–BT and

BNT–BLT–BKT were developed to further improve the piezoelectric properties [5,6].

In spite of a number of reports on the detailed electrical property, however, there are few reports on the microstructure characterizations in BNT–BKT-based piezoceramics, especially in the sub-micrometer scale [7–9]. Considering close correlation between the microstructure and the properties of given materials, an extensive microstructure study is essential for better understanding the materials of our interest and consequently improving the properties more effectively.

In this paper, we reported the microstructure, the electrical properties, and discussed the structure–property relationship of the rhombohedral–tetragonal MPB composition  $0.80\text{BNT}\text{--}0.20\text{BKT}$ . The focus was put on the ferroelectric domain structure and local crystal structure in this sample. The ferroelectric properties in this composition were characterized as well. A complete picture of the structure–property relationship of these systems was demonstrated.

## 2. Experimental procedures

The  $0.80\text{BNT}\text{--}0.20\text{BKT}$  ceramic was prepared by a solid state reaction method from the mixture of  $\text{Bi}_2\text{O}_3$  (99.8%),

\* Corresponding author.

E-mail addresses: [Jackie0712@hotmail.com](mailto:Jackie0712@hotmail.com) (W.-J. Ji), [stzhang@nju.edu.cn](mailto:stzhang@nju.edu.cn) (S.-T. Zhang), [binyang@hit.edu.cn](mailto:binyang@hit.edu.cn) (B. Yang).

$\text{Na}_2\text{CO}_3$  (99.8%),  $\text{K}_2\text{CO}_3$  (98.0%) and  $\text{TiO}_2$  (99.0%). These oxides were mixed in ethanol with carnelian balls by ball-milling for 24 h, then dried and calcined at 800 °C for 2 h and then ball milled again for 24 h. Then these green disks were sintered at 1100 °C for 2 h in covered alumina crucibles. To reduce the evaporation of the volatile elements Bi, Na and K, the disks were embedded in a powder of the same compositions during the sintering.

The structure of ceramic was characterized by X-ray diffraction (XRD, Rigaku Ultima III) and transmission electron microscopy (high-resolution Tecnai F20, TEM). TEM sample was prepared by conventional method. Electrical measurements were carried out on sintered ground disks with silver electrodes. Electrical measurements were carried out at room temperature in silicone oil. Polarization–electric field ( $P$ – $E$ ) and strain–electric field curves ( $S$ – $E$ ) curves were measured by precision premier II (Radiant Tech., USA).

### 3. Results and discussion

Fig. 1(a) shows the XRD pattern of the ceramic. In this paper, the reflections were indexed in pseudo-cubic setting. By scrutinizing the XRD pattern of 0.80BNT–0.20BKT, it can be seen that there are two sets of reflections. The experimental XRD pattern is different from the calculated BNT XRD pattern, which indicates the material is not single phase of BNT. Detail information of the structure will be given by TEM study. We assume there are two phases in this solid material. One can be attributed to the tetragonal structure, the other to the rhombohedral structure. One reflection peak around  $2\theta = 57.0^\circ$  is enlarged, as shown in Fig. 1(b). Peaks typical of the tetragonal and the rhombohedral phases were identified in this figure and therefore leading to the assertion that these two phases co-existing in the 0.80BNT–0.20BKT sample. This observation is in good agreement with results of previous reports [10].

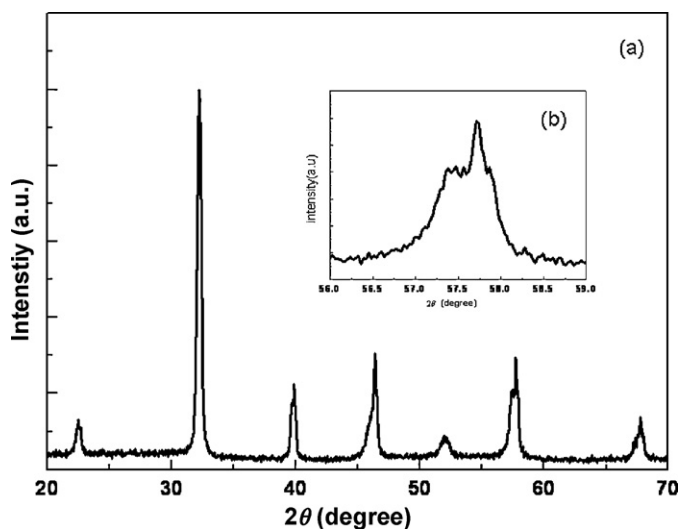


Fig. 1. The XRD pattern of the 0.8BNT–0.2BKT ceramics sintered at 1100 °C for 2 h is shown in (a). One reflection peak around  $2\theta = 57.0^\circ$  is enlarged, as shown in (b).

The ferroelectric domain structures and oxygen octahedron tilting in this composition were characterized by TEM. Fig. 2 is a bright field image of the 0.80BNT–0.20BKT ceramic, which shows a clear stripe structure in the several grains which are indicated by two arrows. The selected area electron diffraction (SAED) pattern taken from bottom left grain is the inset in Fig. 2. The elongation/splitting of high-order reflection spots can be observed, which are demonstrated in the enlarged picture inset in Fig. 2. The splitting of high-order reflection spots is attributed to existence of multi-domains in this grain. Similar phenomena were observed in lead-based ferroelectric ceramics [11,12].

The local crystal structure of this composition was further studied by SAED. It should be stressed that it cannot be unambiguous to determine the space group of these materials due to the tilting-angle limitation in our microscope. But the oxygen octahedron tilting can be determined by the observation of characteristic superlattice in SAED patterns. Both tetragonal (Fig. 3(a) and (b)) and rhombohedral (Fig. 3(c) and (d)) distortions were observed in sample BNT–BKT. As shown in Fig. 3(a) and (b), there are series  $1/2\{h + 1/2, k + 1/2, 0\}$  superlattice reflections besides the basic reflections spots, but only  $1/2\{h + 1/2, k + 1/2, l + 1/2\}$ -superlattice ones in Fig. 3(c) and (d). All indices were labelled in pseudo-cubic setting for the simplicity. In accordance with the Woodward's work [13],  $1/2\{h + 1/2, k + 1/2, l + 1/2\}$  superlattice reflections are the fingerprint of rhombohedral distortion along  $\{111\}$ -axis (denoted as  $a^- a^- a^-$  in Glazer's notation [13]), while  $1/2\{h + 1/2, k + 1/2, 0\}$  ones be tetragonal distortion along  $[001]$ -axis (denoted as  $a^0 a^0 c^+$ ). In other word, the SAED patterns taken from sample BNT–BKT substantiate the co-existence of tetragonal and rhombohedral phases in BNT–BKT sample.

The temperature dependent relative dielectric constant ( $\epsilon_r$ ) and loss tangent ( $\tan \delta$ ) of the composition are shown in Fig. 4(a) and (b), respectively. The frequency dependent depolarization temperature ( $T_d$ ) indicates diffused antiferroelectric–ferroelectric

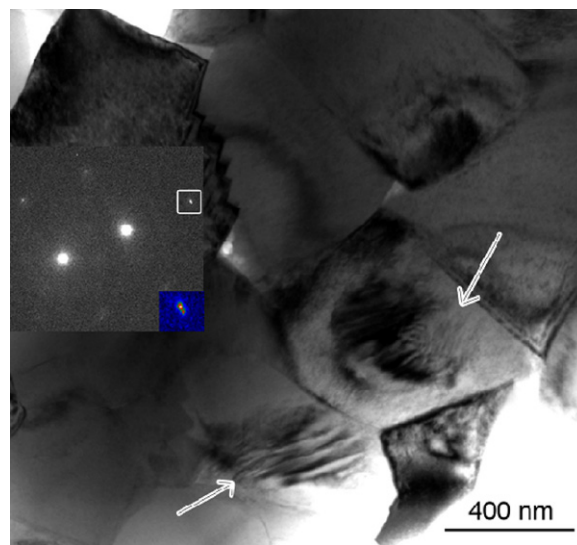


Fig. 2. A bright field TEM image of the 0.8BNT–0.2BKT ceramics. The two arrows indicated the domain structures in the grains. The selected area electron diffraction (SAED) pattern taken from bottom left grain is inset.

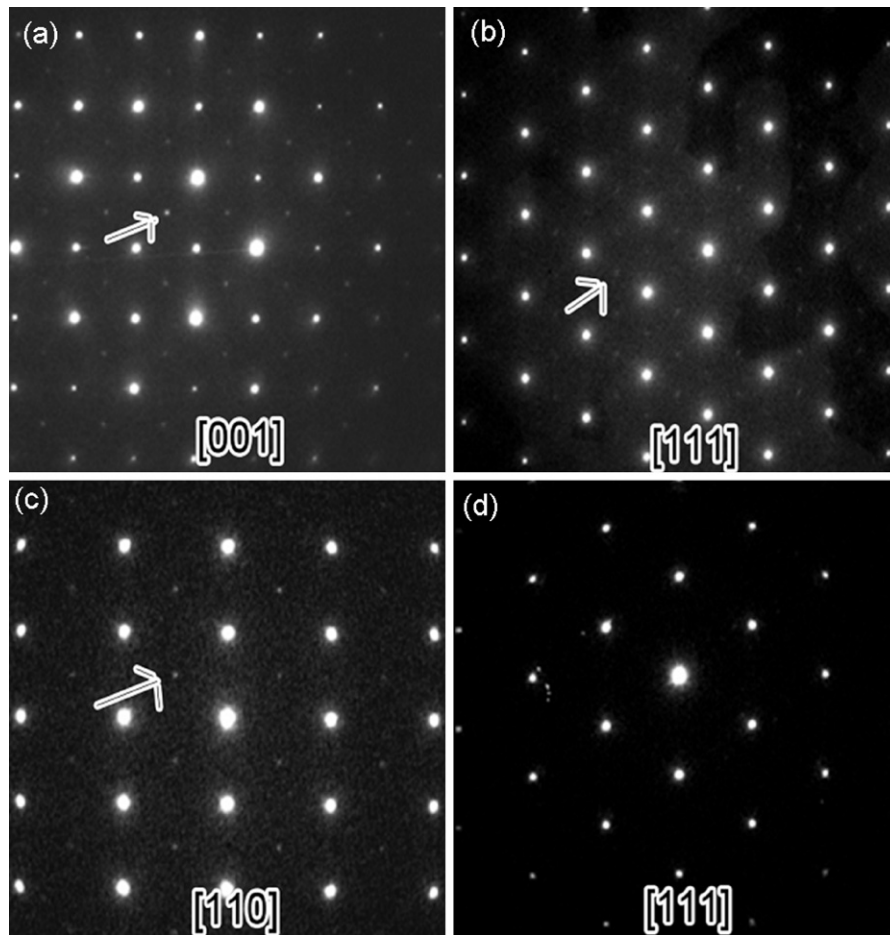


Fig. 3. The selected area electron diffraction (SAED) patterns of the 0.8BNT–0.2BKT ceramics: (a) and (b) show the tetragonal distortions, while (c) and (d) show the rhombohedral distortions.

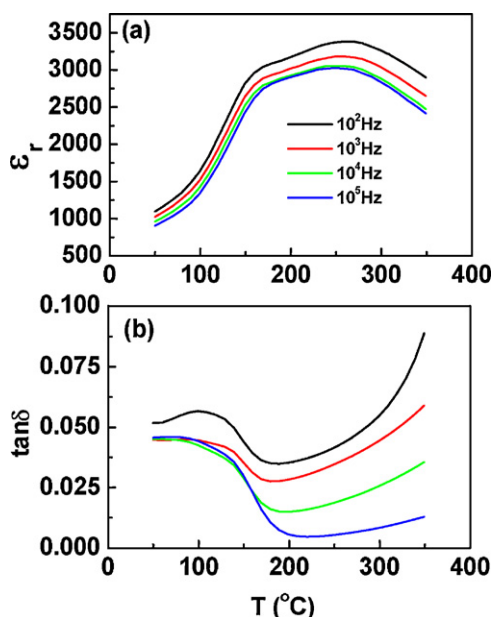


Fig. 4. Temperature dependent (a) relative dielectric constant and (b) loss tangent, the depolarization temperature is determined to be  $\sim 140$  °C.

phase transition, i.e., the ceramics show relaxor ferroelectric characteristics. The  $T_d$  is determined to be  $\sim 140$  °C, consistent with other reports [14].

The room temperature ferroelectric polarization–electric field ( $P$ – $E$ ) hysteresis loop measured under applied field of 6.5 kV/mm is depicted in Fig. 5(a). It is clearly seen that the 0.80BNT–0.20BKT sample exhibits a well-saturated  $P$ – $E$  loop, indicating the ferroelectric nature. The saturated polarization, remnant polarization and coercive field are measured to be  $28.7 \mu\text{C}/\text{cm}^2$ . These polarization and coercive field values are comparable with other reported values for compositions near this rhombohedral–tetragonal MPB region [15] and are also similar to other BNT-rich piezoelectric ceramics [16]. One also can see a butterfly like strain–electric field ( $S$ – $E$ ) curve init shown in Fig. 5(b), which is a fingerprint of ferroelectric materials. With the applied field of 6.5 kV/mm, the maximum total strain and positive strain are observed to be 0.15% and 0.08%, respectively, comparable with literature reports [17]. Both the well saturated  $P$ – $E$  and butterfly shaped  $S$ – $E$  curves are consistent with the above mentioned microstructure characterization that the ceramics have rhombohedral–tetragonal MPB structure with clear ferroelectric domains.

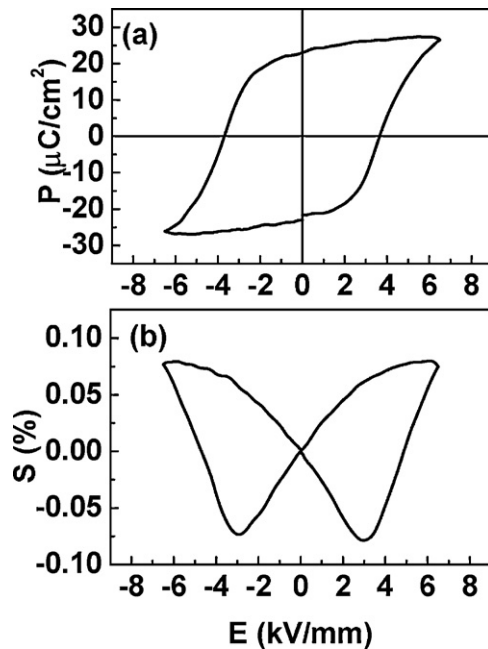


Fig. 5. (a) The polarization–electric field loop, and (b) the strain–electric field curve, of the 0.8BNT–0.2BKT ceramics measured under applied field of 6.5 kV/mm.

#### 4. Conclusion

In conclusion, the rhombohedral–tetragonal MPB composition of 0.80BNT–0.20BKT has been prepared and investigated. X-ray diffraction and electron diffractions results substantiate the co-existence of tetragonal and rhombohedral phases. The ferroelectric domains were clearly observed by electron microscopy, which is further confirmed by the well saturated  $P$ – $E$  hysteresis loop and butterfly  $S$ – $E$  curve. The oxygen octahedron tilting of the samples was studied by SAED. Our results may be helpful not only for further understanding the microstructure–property relationship of BNT–BKT around MPB, but also for further developing high performance BNT–BKT based lead-free piezoelectric ceramics.

#### Acknowledgements

We would like to acknowledge the financial support from the Nation Science Foundation of China (10874069, 50632030 and 10974083), the State key program for basic research

(2007CB613202, 2009CB929503), and the New Century excellent talents in University (NCET-09-0451).

#### References

- [1] V.A. Isupov, Ferroelectric  $\text{Na}_{0.5}\text{Bi}_{0.5}\text{TiO}_3$  and  $\text{K}_{0.5}\text{Bi}_{0.5}\text{TiO}_3$  perovskites and their solid solutions, *Ferroelectrics* 315 (2005) 123–147.
- [2] S.J. Zhang, R. Xia, T.R. Shrout, Lead-free piezoelectric ceramics vs. PZT? *J. Electroceram.* 19 (2007) 251–257.
- [3] J. Rödel, W. Jo, K. Seifert, E.-M. Anton, T. Granzow, D. Damjanovic, Perspective on the development of lead-free piezoceramics, *J. Am. Ceram. Soc.* 92 (2009) 1153–1177.
- [4] A. Sasaki, T. Chiba, Y. Mamiya, E. Otsuki, Dielectric and piezoelectric properties of  $(\text{Bi}_{0.5}\text{Na}_{0.5})\text{TiO}_3$ – $(\text{Bi}_{0.5}\text{K}_{0.5})\text{TiO}_3$  systems, *Jpn. J. Appl. Phys.* 38 (1999) 5564–5567.
- [5] H. Nagata, M. Yoshida, Y. Makiuchi, T. Takenaka, Large piezoelectric constant and high curie temperature of lead-free piezoelectric ceramic ternary system based on bismuth sodium titanate–bismuth potassium titanate–barium titanate near the morphotropic phase boundary, *Jpn. J. Appl. Phys.* 42 (2003) 7401–7403.
- [6] Y. Hiruma, H. Nagata, T. Takenaka, Depolarization temperature and piezoelectric properties of  $(\text{Bi}_{1/2}\text{Na}_{1/2})\text{TiO}_3$ – $(\text{Bi}_{1/2}\text{Li}_{1/2})\text{TiO}_3$ – $(\text{Bi}_{1/2}\text{K}_{1/2})\text{TiO}_3$  lead-free piezoelectric ceramics, *Ceram. Int.* 35 (2009) 117–120.
- [7] C.W. Tai, S.H. Choy, H.L.W. Chan, Ferroelectric domain morphology evolution and octahedral tilting in lead-free  $(\text{Bi}_{1/2}\text{Na}_{1/2})\text{TiO}_3$ – $(\text{Bi}_{1/2}\text{K}_{1/2})\text{TiO}_3$ – $(\text{Bi}_{1/2}\text{Li}_{1/2})\text{TiO}_3$ – $\text{BaTiO}_3$  ceramics at different temperatures, *J. Am. Ceram. Soc.* 91 (2008) 3335–3341.
- [8] V. Dorcet, G. Trolliard, A transmission electron microscopy study of the A-site disordered perovskite  $\text{Na}_{0.5}\text{Bi}_{0.5}\text{TiO}_3$ , *Acta Mater.* 56 (2008) 1753–1761.
- [9] C.W. Tai, Y. Lereah, Nanoscale oxygen octahedral tilting in  $0.90(\text{Bi}_{1/2}\text{Na}_{1/2})\text{TiO}_3$ – $0.05\text{BaTiO}_3$  lead-free perovskite piezoelectric ceramics, *Appl. Phys. Lett.* 95 (2009) 062901.
- [10] Y. Hiruma, K. Yoshii, H. Nagata, T. Takenaka, Phase transition temperature and electrical properties of  $(\text{Bi}_{1/2}\text{Na}_{1/2})\text{TiO}_3$ – $(\text{Bi}_{1/2}\text{A}_{1/2})\text{TiO}_3$  (A = Li and K) lead-free ferroelectric ceramics, *J. Appl. Phys.* 103 (2008) 084121.
- [11] J. Ricote, R.W. Whatmore, D.J. Barber, Studies of the ferroelectric domain configuration and polarization of rhombohedral PZT ceramics, *J. Phys.: Condens. Matter* 12 (2000) 323–337.
- [12] D.I. Woodward, I.M. Reaney, A structural study of ceramics in the  $(\text{BiMnO}_3)_x$ – $(\text{PbTiO}_3)_{1-x}$  solid solution series, *J. Phys.: Condens. Matter* 16 (2004) 8823–8834.
- [13] D.I. Woodward, I.M. Reaney, Electron diffraction of tilted perovskites, *Acta Crystallogr. B* 61 (2005) 387–399.
- [14] K. Yoshi, Y. Hiruma, H. Nagata, T. Takenaka, Electrical properties and depolarization temperature of  $(\text{Bi}_{1/2}\text{Na}_{1/2})\text{TiO}_3$ – $(\text{Bi}_{1/2}\text{K}_{1/2})\text{TiO}_3$  lead-free piezoelectric ceramics, *Jpn. J. Appl. Phys.* 45 (2006) 4493–4496.
- [15] J. Shieh, K.C. Wu, C.S. Chen, Switching characteristics of MPB compositions of  $(\text{Bi}_{0.5}\text{Na}_{0.5})\text{TiO}_3$ – $\text{BaTiO}_3$ – $(\text{Bi}_{0.5}\text{K}_{0.5})\text{TiO}_3$  lead-free ferroelectric ceramics, *Acta Mater.* 55 (2007) 3081–3087.
- [16] Y.P. Guo, Y. Liu, R.L. Withers, F. Brink, H. Chen, Large electric field-induced strain and antiferroelectric behavior in  $(1-x)(\text{Na}_{0.5}\text{Bi}_{0.5})\text{TiO}_3$ – $x\text{BaTiO}_3$  ceramics, *Chem. Mater.* 23 (2011) 219–228.
- [17] T. Takenaka, H. Nagata, Y. Hiruma, Current developments and prospective of lead-free piezoelectric ceramics, *Jpn. J. Appl. Phys.* 47 (2008) 3787–3801.